ACS Macro Letters

Letter

pubs.acs.org/macroletters

Nanofibers from Scalable Gas Jet Process

Rafael E. Benavides,[†] Sadhan C. Jana,*[,†] and Darrell H. Reneker[‡]

Departments of [†]Polymer Engineering and [‡]Polymer Science, The University of Akron, Akron, Ohio 44325-0301, United States

ABSTRACT: A new, simple, and effective method is reported for production of polymer fibers ranging from a few tens of nanometers to a few micrometers from polymer solutions. The method capitalizes on a high velocity expanding gas jet to turn polymer solutions streaming from nozzles into fibers with smooth or wrinkled fiber surface morphology and with core−shell and side-by-side arrangements. The polymer solution is brought in contact with the gas jet on a flat surface, at the tip of a circular needle, and at the surface a pendant drop. The fiber diameter bears relationship with capillary number of the liquid jet and polymer concentration in the solution. Several levels of fiber conglutination are observed as function of collection distance from the nozzle set up.

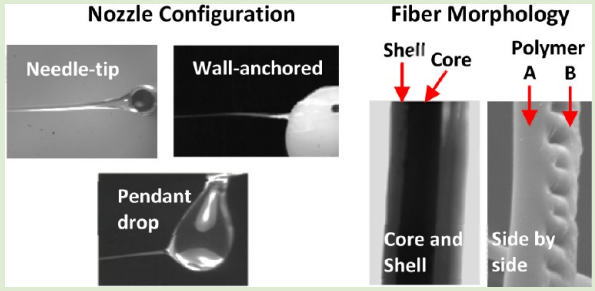

It has become common knowledge that nanofibers present strong gas absorption characteristics due to large surface areas per unit mass, unique surface roughness, and, in some cases, porosity. These attributes can be combined with the intrinsic properties of the polymers, such as biodegradability, crystallinity, and hydrophobic or hydrophilic nature to address an array of suitable applications often limited by low rates of production of nanofibers. Examples include scaffolds for cell growth, wound dressing materials for skin regeneration, industrial thermal and acoustic insulation systems, filtration, fabrication of protective clothing, sensors, and catalytic matrices to name a few.[1−5] Electrospinning has been the preferred method for production of nanofibers and submicrometer fibers from polymeric solutions. However, a relatively low rate of fiber production from a single jet, typically less than 0.3 g/h per jet, high electric voltage necessary to draw the fibers, and a small number of polymer systems amenable to electro-spinning limit more widespread industrial applications.[6−9] Several processes have been considered as high volume alternatives to electro-spinning, such as melt blowing,[10−12] nanofibers by gas jet (NGJ),[13−15] solution blow spinning,[16] or centrifugal spinning or the rotary jet spinning (RJS).[17,18] Nevertheless, these methods have failed to produce submicrometer diameter fiber arrangements with core−shell and side-by-side assembly common in the case of electrospinning process.[19,20]

In this letter, we report a versatile process for production of polymeric fibers with diameter ranging from a few tens of nanometer to a few micrometer in an array of morphological forms and at rates 10−20 times higher than the rate of a single electrospinning jet. The process, termed gas jet nanofibers (GJF), bears several similarities and contrasts with electro-spinning and melt-blowing processes. First, in the GJF process, polymer solutions are extruded as liquid jets from pendant drops or needle tips as in electrospinning. Second, as in melt-blowing, the liquid jet is stretched by the high velocity, expanding compressed gas. Third, the rapid stretching of the liquid jet leads to a cone at the beginning similar to the electrically formed Taylor cone in electrospinning.[21] Fourth, the polymer solution is independently delivered through the nozzles and is brought into contact with high velocity gas. This alleviates concerns of clogging or mechanical constrictions and aids facile adaptation of different fiber configurations, such as of core−shell and side-by-side geometries. A simplified setup of the GJF process consists of a syringe pump, a customized nozzle, a jet of compressed gas, typically air, and a collector, as shown in Figure 1a. The pressure of gas, gravity, viscous force, surface tension, and aerodynamic force all impact the drawing of a single, continuous jet of polymer liquids, as shown in Figure 1b−d from three prototype polymer solution delivery configurations: (i) wall-anchored (Figure 1b) where the solution is allowed to fall under gravity and create a film before the liquid jet is formed, (ii) needle-tip (Figure 1c), and (iii) pendant drop (Figure 1d), formed at the tip of a capillary tube under the influence of surface tension and gravitational forces.

The GJF process is constituted of the following steps. First, the polymer solution is fed into the nozzle and extruded at constant rate by a motorized syringe pump. Single or multiple syringe pumps can be used depending on the number of polymer components used to produce the fibers. Second, the gas and polymer solution are brought in contact depending on the nozzle configuration, for example, wall-anchored as in Figure 1b or a pendant drop at the end of a capillary tube, as in Figure 1d. Third, a liquid jet is initiated by the action of the gas followed by liquid jet stretching and evaporation of the solvent. This process continues until the viscosity of the liquid jet increases due to solvent evaporation to a level that it hinders further stretching and or the velocity of the expanded gas

Received: June 12, 2012
Accepted: July 26, 2012
Published: July 30, 2012

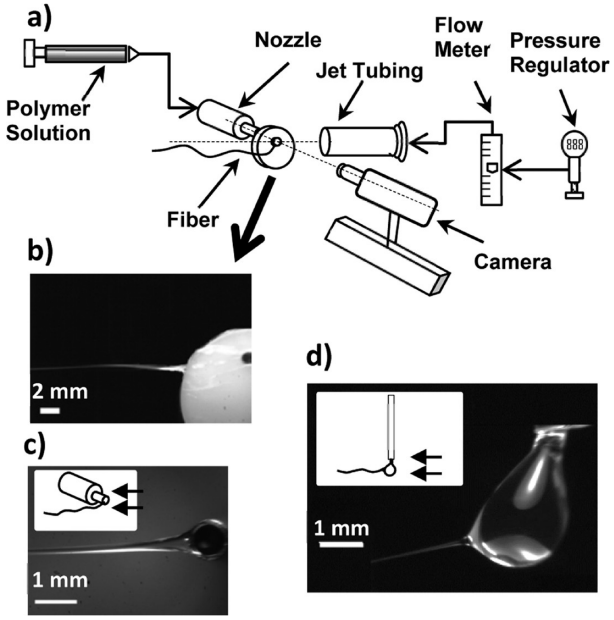

Figure 1. (a) Schematic setup of the GJF process with wall-anchored nozzle. (b–d) Images of polymeric liquid jet emanating from (b) wall-anchored nozzle, (c) needle-tip nozzle, and (d) pendant drop.

equals the velocity of the traveling fiber. Fibers should be collected a few meters from the nozzle to take full advantage of the expanded air jet. As is evident from above, the GJF method is simple to implement.

The capability and feasibility of the GJF process was demonstrated by producing fibers from 6% w/w solution of polyethylene oxide (PEO, M_w = 300000 g/g mol from Alfa Aesar) in ethanol, 6% w/w solution of polyvinyl pyrrolidone (PVP, M_w = 1300000 g/g mol from Alfa Aesar) in ethanol, and 6% w/w solution of polyvinyl acetate (PVAc, M_w = 500000 g/g mol, from Sigma Aldrich) in ethyl acetate, using several nozzles built in-house. Needle-tip nozzles were built from stainless steel needles of internal diameter 0.3–1.22 mm. Wall-anchored nozzle assembly (Figure 1b) was built by attaching 1 mL syringes to flat plastic plates. Glass capillary tubes of 1 mm diameter were used to create pendant drops. The high velocity air jet was created by allowing compressed air to flow through a rigid pipe of internal diameter 11 mm, fitted with a filter, pressure regulator, and a flow meter. The scanning electron microscope (SEM) images of the mats of fibers prepared from the above solutions using a needle-tip nozzle (Figure 1c) of 1.2 mm of internal diameter are presented in Figure 2a–c. Fibers with mean diameter of, respectively, 280, 186, and 425 nm were obtained for PEO, PVP, and PVAc using compressed air jet with 40 psi pressure and solution feeding rate of 0.8 mL/min. Several processing variables can be adjusted to create significant changes in the fiber mean diameter and morphology. These include air jet pressure, distance between the nozzles for polymer solution and the air jet, volumetric rate of polymer solution, and the distance from the nozzle where the polymer fibers are collected. Figure 2d presents SEM images of PVP fibers obtained from 10% w/w solution in ethanol using the needle-tip nozzle at a feeding rate of 0.8 mL/min and different air jet pressures. As is evident, an increase of the air jet pressure

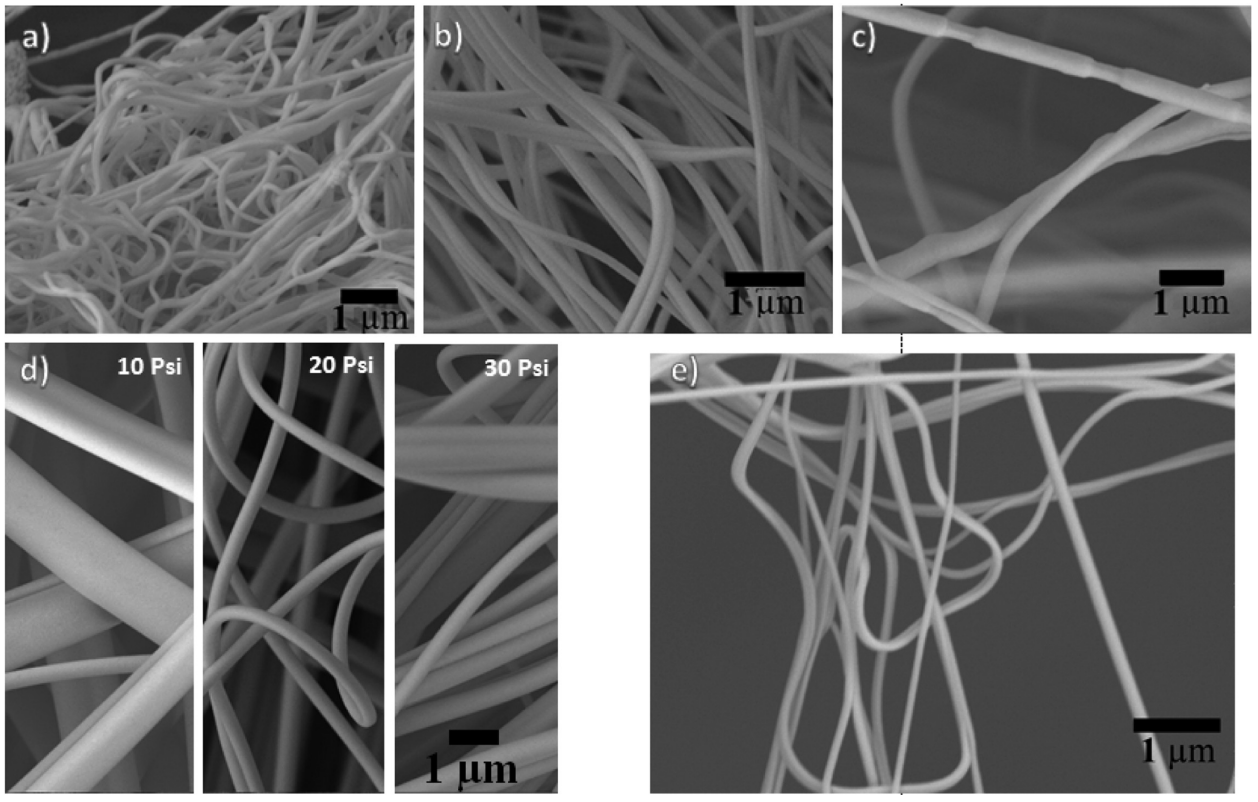

Figure 2. SEM micrographs of fibers produced from solutions of (a) PEO 6% w/w in ethanol, (b) PVP 6% w/w in ethanol, (c) PVAc 6% w/w in ethyl acetate, (d) PVP 10% w/w at three pressures of gas jet (see values at the top of each image) using a needle-tip nozzle of 1.2 mm of internal diameter, and (e) PVP 2% w/w in ethanol.

dx.doi.org/10.1021/mz300297g | *ACS Macro Lett.* 2012, 1, 1032–1036

Table 1. Effect of Processing Variables on Fiber Diameter and Morphology Obtained by GJF Process[a]

polymer and mol wt	conc wt %	air pressure (psi); air flow rate (m^3/min)	collection distance (m)	mean fiber diameter (μm)	nozzle type	fiber characteristics	solid polymer feeding rate (g/h)
PEO 1 M	3.5	10; 0.1556	1.8	3.6	needle-tip	fiber	1.7
PEO 1 M	3.5	20; 0.1339	1.8	1.7	needle-tip	fiber	1.7
PEO 1 M	3.5	30; 0.12	1.8	1.2	needle-tip	fiber	1.7
PEO 1 M	3.5	40; 0.1081	1.8	0.8	needle-tip	fiber	1.7
PEO 300 K	3	15; 0.1422	1.8	0.2	wall-anchored	fiber	1.4
PEO 300 K	3	15; 0.1422	1.8	0.2	needle-tip	fiber	1.4
PEO 1 M	3	10; 0.1556	1.8	0.2	pendant drop	fiber	0.09
PVP 1.3 M	6	10; 0.1556	1.8	0.2	wall-anchored	fiber	2.9
PVP 1.3 M	6	20; 0.1339	1.8	0.4	wall-anchored	fiber	5.7
PVP 1.3 M	6	30; 0.12	1.8	0.6	wall-anchored	fiber and bead	8.6
PVP 1.3 M	2	20; 0.1339	1.8	0.1	wall-anchored	fiber and bead	0.9

[a]Polymer molecular weight 1 M = 1000000; 300 K = 300000, 1.3 M = 1300000. Needle-tip nozzle diameter Ø = 0.83 mm. Air flow rate is in cubic meter per min at 20 °C and at pressure indicated in the table.

from 10 to 30 psi caused a reduction of the number average mean diameter of the fibers from 1.6 to 0.34 μm. The same nozzle allowed an increase of the volumetric flow rate of solution to 1.6 mL/min without significant changes in the fiber diameter. A further increase of solution flow rate resulted in the formation of solid beads along the fiber. Fibers of a few tens of nanometer were produced using a low concentration of polymers in solution; a 2% w/w PVP solution in ethanol led to fibers of 60 nm mean diameter (Figure 2e). The PEO fibers obtained in the GJF process showed a diameter comparable to electrospinning.[22] Table 1 presents a summary of the effects of several processing variables on fiber diameter and morphology. It is seen that there is no significant difference between the fibers produced using a wall-anchored nozzle (Figure 1b) or a needle-tip nozzle (Figure 1c) if process parameters are similar. On the other hand, the nozzle configuration based on pendant drops (Figure 1d) gave rise to fibers with a much smaller mean diameter (~200 nm) at low air jet pressures of 10 psi. At a higher pressure of the air jet the pendent drop became unstable.

The fiber conglutination, necessary to create three-dimensional webs, was achieved by collecting fibers closer to the liquid jet. Figure 3 shows three different degrees of conglutination of PEO fibers produced using a wall-anchored nozzle system (Figure 1b) and air jet pressure of 10 psi; fibers were collected at specified distances from the inception of the liquid jet.

The performance of the GJF process, especially the ability to form stable and continuous jets of polymer solutions, is dictated by the polymer solution properties, such as concentration (C), viscosity (μ), and surface tension (γ), as in the electrospinning process.[23] The mean diameter of the fibers is known to decrease with a reduction of viscosity or reduction of concentration of the polymer in solution. The lower limit of polymer concentration is dictated by the critical concentration C^* for achieving polymer chain entanglement.[24] In this context, the capillary number (Ca) of the extended liquid jet relates the viscous stress with the interfacial stress, $Ca = \mu V/\gamma$, where μ,V, and γ are the values of viscosity, velocity of the liquid jet, and surface tension of the polymer solution, respectively. For systems with a low capillary number, for example, for surface tension dominating, the jets underwent early break-up due to

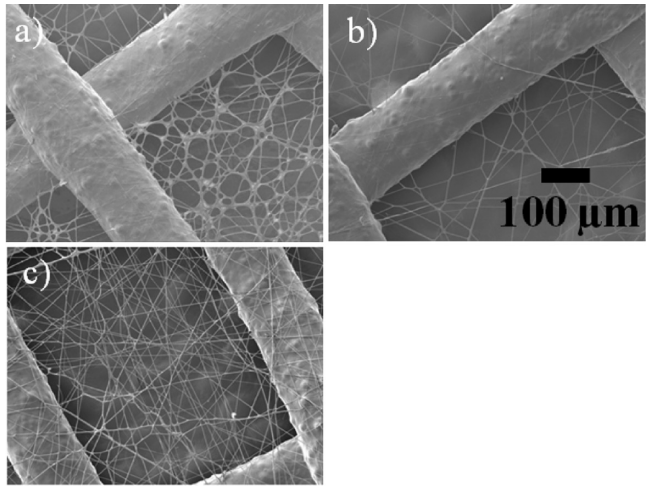

Figure 3. Different conglutination levels of PEO fibers collected at different distances from the nozzle: (a) 10, (b) 50, and (c) 100 cm.

Rayleigh instability[25] and often lead to beaded fibers. Smooth fibers are produced at moderate values of Ca, achieved by increasing the polymer solution viscosity or the velocity of the liquid jet. At very high values of Ca, the fibers show defects induced by the turbulent nature of the gas flow. These cases are schematically presented in Figure 4.

The fibers with side-by-side and core−shell morphological forms were produced by the GJF process easily using fabricated prototype nozzles. A wall-anchored nozzle system (Figure 1b) was modified to include two polymer streams, as shown in Figure 5a. In this case, polymer solution A (red color) is allowed to flow over polymer solution B (blue color) forming a stratified two-layer falling liquid stream before an air jet turns the stream into a liquid jet. In this manner, fibers with side-by-side morphology of mean diameter 0.8 μm were obtained from a solution of PEO 6% w/w in ethanol and PVP 6% w/w in ethanol at a feed rate of 0.4 mL/min for each solution and air jet pressure of 20 psi (Figure 5c). The same prototype nozzle was used to produce fibers from immiscible polymer systems, such as PVAc 6% w/w in ethyl acetate and PEO 6% w/w in ethanol, as shown in Figure 5d. The side-by-side fused fibers of

dx.doi.org/10.1021/mz300297g | ACS Macro Lett. 2012, 1, 1032−1036

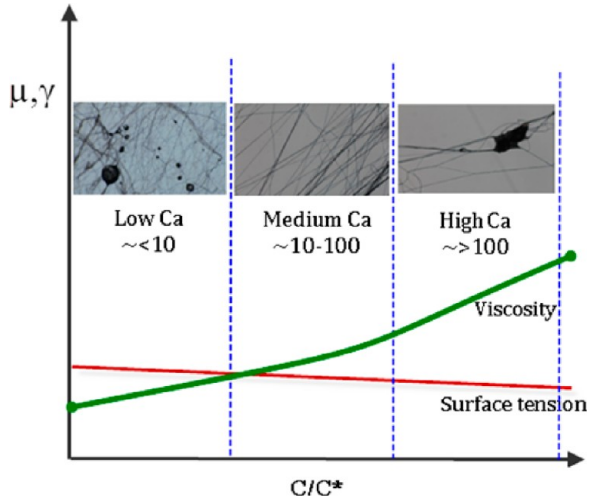

Figure 4. Schematic showing the dependence of polymer solution viscosity (μ) and surface tension (γ) on polymer concentration ratio (C/C^*). Also presented are images of the fibers obtained from a needle-tip nozzle at various values of capillary number.

immiscible polymers PVAc and PEO seen in Figure 5d demonstrate the possibilities of combining other immiscible polymers into nanofibers. However, the polymer systems and the solvents should be carefully selected to avoid the possibilities of premature solvent evaporation and polymer precipitation.

The set of immiscible and miscible polymers can also be converted into nanofibers of core−shell morphology by the coaxial feeding arrangement (syringe-in-syringe technique) shown in Figure 5b. The process also allows incorporation of nanoparticles into polymer solutions. A solution of 6% w/w of PEO and trisilanol isobutyl polyhedral oligomeric silsesquioxane (POSS) particles (1:3 ratio) in ethanol was converted into fibers (Figure 5e). The self-assembly of POSS molecules in the polymer[26] led to rough surface morphology of the fibers. Smooth fibers (Figure 5f) were obtained when the PEO/POSS solution was kept in the core and a solution of PVAc 6% w/w in ethyl acetate was kept as the shell (Figure 5b) with a feeding ratio of 1:2 w/w. Core−shell fibers from other polymer systems were also produced; Figure 5g presents transmission electron microscope image of fibers with ~620 nm diameter core of PVP and shell of PEO.

We have demonstrated the ability of the GJF process to produce fibers of a diameter ranging from tens of nanometers to a few micrometer using a single or multiple polymers, either miscible or immiscible, and polymers filled with nanoparticles. The GJF process utilizes a balance of the forces originating from viscous, surface tension, and aerodynamic sources. The method uses scalable and independent gas and liquid delivery systems and produces fibers at high rates. The fiber diameter distribution, porosity, and conglutination can be conveniently tailored to target specific applications. The simplicity of the process and the nozzle designs allow production of a variety of nanofiber morphologies so far obtained from electrospinning or vapor grown processes. Nozzles with customized designs are easily fabricated for testing of prototypes.

AUTHOR INFORMATION

Corresponding Author

*E-mail: janas@uakron.edu.

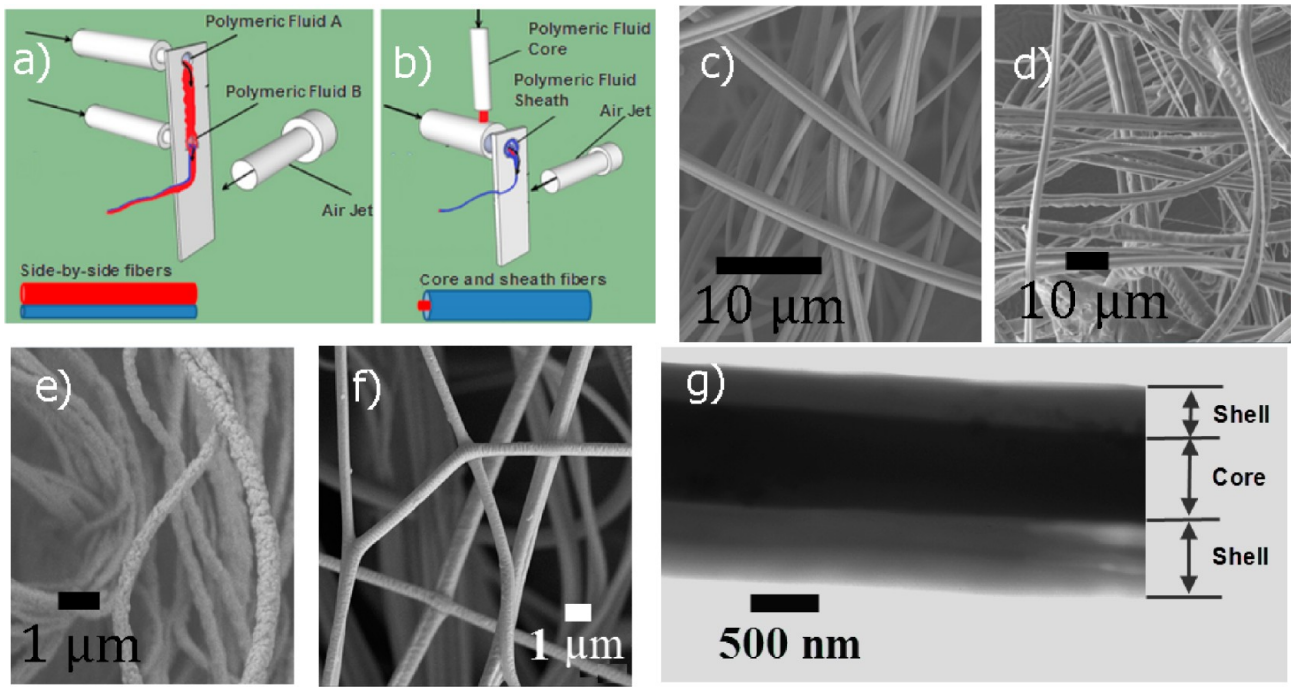

Figure 5. (a, b) Schematic of wall-anchored nozzles to produce fibers with (a) side-by-side and (b) core−shell morphology. (c−f) SEM images showing various morphological forms of fibers. (c) Side-by-side using 6% w/w PEO in ethanol and PVP 6% w/w in ethanol. (d) Side-by-side from PVAc 6% w/w in ethyl acetate, and PEO 6% w/w in ethanol. (e) Blend of PEO and trisilanol isobutyl POSS in ethanol. (f) Core and shell using blend of PEO and trisilanol isobutyl POSS in core and PVAc in shell. (g) Transmission electron micrograph showing PVP core and PEO shell in a section of the fiber. The diameter of the nozzle tip was 0.83 mm. The distance between the center lines of the two nozzles in (a) was kept at 18 mm to produce side-by-side fibers.

dx.doi.org/10.1021/mz300297g | *ACS Macro Lett.* 2012, 1, 1032−1036

Notes

The authors declare no competing financial interest.

REFERENCES

(1) Dersch, R.; Steinhart, M.; Boudriot, U.; Greiner, A.; Wendorff, J. H. *Polym. Adv. Technol.* **2005**, *16* (2−3), 276−282.
(2) Deitzel, J. M.; Kleinmeyer, J.; Harris, D.; Beck Tan, N. C. *Polymer* **2001**, *42* (1), 261−272.
(3) Dzenis, Y. *Science* **2004**, *304* (5679), 1917−1919.
(4) Pham, Q. P.; Sharma, U.; Mikos, A. G. *Tissue Eng.* **2006**, *12* (5), 1197−1211.
(5) Huang, Z.-M.; Zhang, Y. Z.; Kotaki, M.; Ramakrishna, S. *Compos. Sci. Technol.* **2003**, *63* (15), 2223−2253.
(6) Bhardwaj, N.; Kundu, S. C. *Biotechnol. Adv.* **2010**, *28* (3), 325−347.
(7) Greiner, A.; Wendorff, J. H. *Angew. Chem., Int. Ed.* **2007**, *46* (30), 5670−5703.
(8) Li, D.; Xia, Y. *Adv. Mater.* **2004**, *16* (14), 1151−1170.
(9) Reneker, D. H.; Yarin, A. L.; Zussman, E.; Xu, H. Electrospinning of Nanofibers from Polymer Solutions and Melts. In *Advances in Applied Mechanics*; Hassan, A.; Erik van der, G., Eds. Elsevier: New York, 2007; Vol. *41*, pp 43−346.
(10) Pinchuk, L. S. *Melt Blowing: Equipment, Technology, And Polymer Fibrous Materials*; Springer: Berlin; New York, 2002; p xii, p 212.
(11) Kayser, J. C.; Shambaugh, R. L. *Polym. Eng. Sci.* **1990**, *30* (19), 1237−1251.
(12) Ellison, C. J.; Phatak, A.; Giles, D. W.; Macosko, C. W.; Bates, F. S. *Polymer* **2007**, *48* (11), 3306−3316.
(13) Reneker, D. H. Process and Apparatus for the Production of Nanofibers. Patent *6520425*, 2003.
(14) Reneker, D. H. Process and Apparatus for the Production of Nanofibers. Patent *6695992*, 2004.
(15) Reneker, D. H.; Chun, I.; Ertley, D. Process and Apparatus for the Production of Nanofibers. Patent *6382526*, 2002.
(16) Medeiros, E. S.; Glenn, G. M.; Klamczynski, A. P.; Orts, W. J.; Mattoso, L. H. C. *J. Appl. Polym. Sci.* **2009**, *113* (4), 2322−2330.
(17) Badrossamay, M. R.; McIlwee, H. A.; Goss, J. A.; Parker, K. K. *Nano Lett.* **2010**, *10* (6), 2257−2261.
(18) Weitz, R. T.; Harnau, L.; Rauschenbach, S.; Burghard, M.; Kern, K. *Nano Lett.* **2008**, *8* (4), 1187−1191.
(19) McCann, J. T.; Li, D.; Xia, Y. *J. Mater. Chem.* **2005**, *15* (7), 735−738.
(20) Gupta, P.; Wilkes, G. L. *Polymer* **2003**, *44* (20), 6353−6359.
(21) Taylor, G. *Proc. R. Soc. A* **1969**, *313* (1515), 453−475.
(22) Fong, H.; Chun, I.; Reneker, D. H. *Polymer* **1999**, *40* (16), 4585−4592.
(23) Eggers, J. *Rev. Mod. Phys.* **1997**, *69* (3), 865−930.
(24) Shenoy, S. L.; Bates, W. D.; Frisch, H. L.; Wnek, G. E. *Polymer* **2005**, *46* (10), 3372−3384.
(25) Papageorgiou, D. T. *Phys. Fluids* **1995**, *7* (7), 1529−1544.
(26) Roy, S.; Feng, J.; Scionti, V.; Jana, S. C.; Wesdemiotis, C. *Polymer* **2012**, *53*, 1711−1724.